International Journal of Chemical, Materials and Biomolecular Sciences
ISSN: 2415-6620
Vol:8, No:9, 2014

Rheological and Thermomechanical Properties of Graphene/ABS/PP Nanocomposites

Marianna I. Triantou, Konstantina I. Stathi, Petroula A. Tarantili

***Abstract*—**In the present study, the incorporation of graphene into blends of acrylonitrile-butadiene-styrene terpolymer with polypropylene (ABS/PP) was investigated focusing on the improvement of their thermomechanical characteristics and the effect on their rheological behavior. The blends were prepared by melt mixing in a twin-screw extruder and were characterized by measuring the MFI as well as by performing DSC, TGA and mechanical tests. The addition of graphene to ABS/PP blends tends to increase their melt viscosity, due to the confinement of polymer chains motion. Also, graphene causes an increment of the crystallization temperature (T_c), especially in blends with higher PP content, because of the reduction of surface energy of PP nucleation, which is a consequence of the attachment of PP chains to the surface of graphene through the intermolecular CH-π interaction. Moreover, the above nanofiller improves the thermal stability of PP and increases the residue of thermal degradation at all the investigated compositions of blends, due to the thermal isolation effect and the mass transport barrier effect. Regarding the mechanical properties, the addition of graphene improves the elastic modulus, because of its intrinsic mechanical characteristics and its rigidity, and this effect is particularly strong in the case of pure PP.

***Keywords*—**Acrylonitrile-butadiene-styrene terpolymer, blends, graphene, polypropylene.

I. Introduction

AMONG the polyolefins, isotactic polypropylene (PP) is one of the most useful and versatile polymers, suitable for a wide range of applications [1]. PP has poor impact strength and high molding shrinkage, but it is lightweight and it has high elongation, as well as, good chemical resistance, high heat distortion temperature, good processability and economic merits. On the contrary, acrylonitrile-butadiene-styrene (ABS) terpolymer shows poor elongation accompanied with high impact strength [2]-[4]. Therefore, blending of PP with ABS would be desirable to achieve higher impact strength without sacrificing important properties of PP, which would significantly increase its scope of applications [1], [2].

Markin and Williams [5] investigated the morphology and the mechanical properties of ABS/PP blends. Gupta et al. [6] studied the effect of blending ratio, shear stress and shear rate on flow properties, melt viscosity and melt elasticity of PP/ABS and PP/ABS/LDPE (low-density polyethylene) blends. In addition, they correlated the structure and morphology with the mechanical properties of PP/ABS and PP/ABS/LDPE blends [7]. Shu et al. [8] studied the formation of β-PP in the PP/ABS blends and the effects of phase composition and thermal conditions on the β-PP formation in the PP/ABS blends, whereas Wang et al. [9] studied the effect of ABS on the β-nucleation of PP as well as on the crystallization and melting behavior of β-PP/ABS blends.

In order to improve the compatibility between the two polymers, Frounchi and Burford [10] prepared 80/20 and 20/80 PP/ABS blends modified with 5 wt% styrene-butadiene-stryrene (SBS), styrene-isoprene-styrene (SIS), styrene-ethylene-butadiene-styrene (SEBS) and maleated functionalized SEBS (SEBS-g-MAH). Also, Arroyo et al. [11] added 0-10 wt% SBS into 75/25, 50/50 and 25/75 PP/ABS blends, in order to test it as a compatibilizer. The above authors observed a more uniform morphology, as well as an increase of toughness (elongation and impact strength).

Lee et al. [12] added SEBS and SEBS-g-MAH in PP/ABS 70/30 w/w blends. They recorded an improvement of impact strength with minimal tensile strength loss and a smaller droplet size by the addition of SEBS-g-MAH and they concluded that MAH plays an important role as impact modifier and compatibilizer, possibly because of the generation of dipolar interactions with polar group in ABS. In a previous study [3], the same research team had incorporated polypropylene grafted maleic anhydride (PP-g-MAH) in PP/ABS 70/30 w/w blends and observed an increase in impact, tensile and flexural strength with the addition of 3 phr PP-g-MAH. At this amount, the droplet size of the ABS phase in ABS/PP blends shows the minimum value whereas the complex viscosity gained the highest value. The decrease in droplet size suggests an increase of compatibility between the PP and ABS, since the decrease of the droplet size in polymer blend is related with the decrease of the interfacial tension between the two polymers. Earlier [13], they had investigated the addition of PP grafted styrene-acrylonitrile copolymer (PP-g-SAN) in PP/ABS blends and they had reported an increase in tensile strength for the whole composition range, when PP-g-SAN is added at 3 phr, as well as an increase of flexural and impact strength in PP-rich compositions.

Patel et al. [14] used PP-g-2-hydroxyethyl methacrylate (2-HEMA) as a compatibilizer for PP/ABS blends and observed better homogeneity and finer distribution of the dispersed phase and an improvement in the mechanical properties, particularly in PP-rich blends. A concentration of compatibilizer of 2.5 phr was found to be critical for the improvement of mechanical properties. In a previous work [2],

M. I. Triantou and K. I. Stathi are with the National Technical University of Athens, Zographou, 15780 Greece (e-mail: mtriantou@teemail.gr, konstantinastathi@yahoo.gr).

P. A. Tarantili is with the National Technical University of Athens, Zographou, 15780 Greece (phone: +30 2107723289; fax: +30 2107723163; e-mail: taran@chemeng.ntua.gr).

they had incorporated PP-g-acrylic acid in PP/ABS blends. The use of PP-g-acrylic acid brings about an improvement in the Izod impact strength, tensile strength and tensile modulus of PP/ABS blends. A 5% concentration of compatibilizer is the optimum for the improvement in these properties. Furthermore, the compatibilization of blends results in a smaller size distribution of the dispersed phase (ABS) in PP-rich blends.

It has been reported that organoclays can contribute to compatibility of blends of immiscible polymers, acting as linkages between the two phases by embedding in both of them and, hence, improve their properties [15]-[17]. Sung et al. [18] observed that in 70/30 ABS/PP nanocomposite, the clay is mostly located in the ABS matrix because of its good affinity with ABS. Also, the size of the PP droplet is decreased with clay content, for concentrations up to 4 phr. The morphology of the dispersed PP phase changes from droplet to droplet/elongated with the increase of clay's content. This change is attributed to the location of clay in the continuous phase of ABS which causes increase of viscosity of ABS phase and decrease of the viscosity ratio of the PP and the continuous phase of ABS.

The combined action of compatibilizer (PP-g-MAH) and organoclay was studied by Xiang-fang et al. [4], who observed that PP-g-MAH not only improves the compatibility of PP/ABS, but also promotes the dispersion of nanoparticles in the continuous phase of PP and dispersed phase of ABS. In addition, nanoparticles can reduce the rate of crystallization and increase the degree of crystallinity, because of their similar polarity with the polymeric matrix.

Recently, conductive composites gained a wide attention in the scientific and in the industrial community because of the possibility of exploiting their unique properties in various applications, as electromagnetic interference shielding, electrostatic dissipation and gas sensors. Among all the conductive fillers, namely, carbon black or carbon fibers, carbon nanotubes (CNTs) were found to be more promising because of their unique electrical properties with high aspect ratio [19]. Khare et al. [20] studied the effect of compatibilizer (PP-g-MAH and styrene MA) and modifier on morphology and electrical conductivity of 45/55 PP/ABS blends containing multiwall carbon nanotube (MWNT). In a previous study [21], they showed that MWNT can act like a compatibilizer resulting in refinement in the morphology, whether I particulate dispersion or co-continuous structure. Lower electrical percolation threshold was observed in continuous 45/55 blends. Moreover, the melt viscosity of blends constituents was observed to play an important role on controlling the dispersion of MWNT in a specific phase.

The latest family of nanomaterials proposed as additives for improvement polymer property balances are based on graphene. Graphite is found naturally in the form of flakes, which are composed of layers less than 100 nm thick. Each layer is divided in aggregates of graphene sheets with about 1-2 nm thick. The spacing of the aggregates is between 7 and 16 Å and the distance between the sheets is 3.35 Å. Graphene sheets are bound by Van der Waals forces and each sheet is composed of hybridized sp^2 carbon atoms in a hexagonal structure [22], [23]. The in-plane covalent bonds between the carbon atoms of graphene sheets are much stronger with respect to the weak bonds between the carbon atoms of adjacent graphene sheets [24]. Graphene is considered preferential over some conventional fillers, exhibiting lower fabricating cost in comparison with carbon nanotubes (CNTs) and being more environmentally friendly compared to the modified organo-montmorillonite (OMMT) [25]. It presents a combination of high thermal, mechanical, electrical and optical properties, as well as a high aspect ratio [26]-[29]. These properties make graphene suitable for developing conductive nanocomposites, which could be useful in electronic circuits, sensors and actuators [26], [30]. Graphene has already been showing promise for applications, such as transistors, transparent electrodes, liquid crystal devices, ultra-capacitors and ultra-tough paper [31], as well as batteries, hydrogen storage systems, solar cells and spintronics [32].

The incorporation of such materials in polymeric matrices produces nanocomposites with improved properties [23]. For example, Heo et al. [33] used graphene, functionalized with octadecylamine, in ABS matrix and observed great improvement of its thermomechanical properties.

The addition of graphene in PP matrix has already been studied by several authors. In order to prepare graphene/PP nanocomposites, in situ polymerization [25], [30], [34], [35], solution blending [36] and melt mixing [32], [37]-[39] have been used.

However, the effect of incorporation of graphene in pure ABS or PP has been studied; its effect on the morphology and properties of ABS/PP blends has not been studied yet. Therefore, the aim of the present research is to focus on how graphene affects the rheological behavior and thermomechanical characteristics of ABS/PP blends.

II. Experimental

A. Materials

The terpolymer poly(acrylonitrile – butadiene – styrene) (ABS), was supplied by BASF, under the trade name Terluran® GP-35, whereas the polypropylene (Ecolen® HZ40P) was donated by Hellenic Petroleum SA. Graphene with the trade name GRAFEN®-iGP2, supplied by Grafen Chemical Industries Co., was incorporated as reinforcing nanofiller into ABS/PP blends, at a concentration of 2 phr.

B. Preparation of Nanocomposites

ABS/PP blends with compositions: 100/0, 70/30, 50/50, 30/70 and 0/100 (w/w) were prepared by melt mixing, in a co-rotating twin-screw extruder, with L/D=25 and 16 mm diameter (Haake PTW 16). The rotational speed of screws was 200 rpm. The extruder was heated at five zones along the cylinder and the die. The temperature profiles of the barrel from the hopper to the die were 190-195-195-200-200-205°C for ABS, 180-180-185-185-190-190°C for PP and 190-190-195-195-200-200°C for ABS/PP blends. All materials were dried before processing, in order to prevent hydrolytical

degradation. After melt mixing, the obtained material in the form of continuous strands was granulated using a Brabender knife pelletizer.

C. Characterization

The Melt Flow Index (MFI) measurements were carried out according to ASTM D 1238 specification, in a Kayeness Co. model 4004 capillary rheometer at 230°C with 2.16 kg load.

Differential Scanning Calorimetry (DSC) measurements were run in a Mettler Toledo model DSC 1 differential scanning calorimeter. 8–10 mg from each sample were heated from 30 to 200°C to erase previous thermal history and then cooled to 30°C and heated again to 200°C at a rate of 10°C/min under nitrogen flow.

The structural crystallinity of PP and its blends was evaluated in a Siemens 5000 apparatus X-ray diffractometer (40kV, 30mA) using CuKα irradiation with a wavelength of λ=0.154 nm. The diffractograms were scanned in the 2θ range from 2-40° with rate of 0.02 °/sec. Samples for X-ray analysis were obtained from compression molded plaques.

Thermogravimetric analysis (TGA) was performed in a Mettler Toledo (TGA-DTA model) thermal gravimetric analyzer. The tests were run with samples of 8-10 mg from 25 to 600°C, at a heating rate of 10°C/min, in nitrogen atmosphere.

Mechanical property testing of injection molded tensile specimens was carried out according to ASTM D 638, in an Instron tensometer (4466 model), operating at grip separation speed of 50 mm/min. Injection moulding was performed with an ARBURG 221 K ALLROUNDER machine. The mould was a two-cavity system capable of producing dump-bell specimens with the appropriate dimensions. For ABS, the temperature profile was: 260-260-260-260-265°C, with 1000 and 1150 bar injection pressures and 500 bar back pressure. For all the other ABS/PP blends, the temperature profile was: 190-190-190-195-195°C, with 1400 and 1350 bar injection pressures and 600 bar back pressure.

III. Results and Discussion

From the data presented in Table I, it can be observed that ABS exhibits a significantly lower melt flow index (MFI) as a result of its higher melt viscosity in comparison with PP. The ABS/PP blends present melt behavior closer to that of PP. Moreover, the melt viscosity of ABS/PP blend is decreased slightly with increasing PP content.

TABLE I
Melt Flow Index Values of ABS/PP Blends

Graphene (phr)	MFI (g/10 min)				
	ABS/PP (w/w)				
	100/0	70/30	50/50	30/70	0/100
0	0.88 ±0.06	8.90 ±0.49	11.54 ±0.31	11.71 ±0.25	13.62 ±0.47
2	1.12 ±0.06	7.35 ±0.43	10.14 ±0.25	10.97 ±0.25	12.74 ±0.58

The incorporation of graphene into ABS/PP blends results in a slight decrease of their melt flow index, compared to that of no reinforced blends at all the examined compositions, except that of neat ABS. This decrease in flow index is a result of the increase of the system's viscosity. This effect can be attributed to the confinement of the polymer chains mobility caused by graphene nanosheets.

The ABS/PP blend consists of the following three phases; polybutadiene (PB), styrene-acrylonitrile (SAN) copolymer phase and polypropylene (PP). However, only the glass transition temperature (T_g) of stryrene-acrylonitrile phase was determined by differential scanning calorimetry. The composition of ABS/PP blend, as well as the incorporation of graphene, does not seem to have any significant effect on the glass transition temperature (T_g) of SAN phase as it can be seen from the results in Table II. This might be reasonable, because of the poor miscibility between the two polymers and the lack of interactions between graphene and polymeric chains. A strong interfacial bonding could hinder the mobility of polymeric chains as well as their vibrational motion through T_g region more effectively [40]. In order to increase the affinity between filler and polymers, Heo et al. [33] functionalized graphene by octadecylamine and observed an increase of glass transition temperature (T_g) of ABS with increasing filler content from 0 to 1 wt%. The interpretation of this effect was a corresponding increase in crosslink density, as well as the restriction of the segmental relaxation of chain segments near graphene sheets. Further increase of graphene concentration leads to a decrease of T_g, due to the graphene's agglomeration.

TABLE II
Thermal Transitions of ABS/PP Blends

Graphene (phr)	ABS/PP (w/w)				
	100/0	70/30	50/50	30/70	0/100
	T_g (°C)				
0	105.0 ±0.09	105.4 ±0.70	105.4 ±0.88	104.9 ±0.48	-
2	104.4 ±0.01	104.4 ±0.71	105.3 ±0.61	105.5 ±0.41	-
	T_m (°C)				
0	-	164.0 ±0.71	163.3 ±0.28	163.5 ±0.39	164.6 ±1.13
2	-	163.5 ±0.34	164.3 ±0.11	164.3 ±0.67	164.8 ±0.38
	T_c (°C)				
0	-	116.5 ±0.20	117.1 ±0.24	116.5 ±0.70	113.8 ±1.34
2	-	118.3 ±0.09	119.8 ±0.82	121.6 ±0.49	125.2 ±0.54
	ΔH_m (J/g)				
0	-	32.14 ±1.44	45.95 ±0.65	64.03 ±0.70	93.48 ±1.02
2	-	31.26 ±0.58	47.54 ±0.82	61.95 ±1.75	93.35 ±1.97
	ΔH_c(J/g)				
0	-	34.42 ±1.14	47.81 ±1.33	65.72 ±0.81	95.40 ±1.00
2	-	29.20 ±0.81	47.97 ±0.17	62.41 ±1.87	91.92 ±1.28

Furthermore, as it can be seen from Table II, the melting temperature (T_m) of ABS/PP blends is not affected by its composition or by the addition of graphene nanosheets. The

melting enthalpy (ΔH_m) increases with increasing PP loadings in ABS/PP blend. The addition of graphene in ABS/PP blends does not essentially influence the melting enthalpy.

Moreover, from the results of the above table it is observed that the crystallization temperature (T_c) of ABS/PP blend is slightly higher than that of pure PP. The incorporation of graphene to ABS/PP blends shifts their crystallization temperature to higher values. This increase is more intense as the PP content in the ABS/PP blend increases, which suggests that graphene platelets promote the crystallization of PP by acting as nucleating agents. The isotactic PP (iPP) chains may be attached to the surfaces of the carbon nanofiller through the intermolecular CH-π interaction between iPP and the carbon filler; as a result, the surface energy of iPP nucleation can be reduced and, thus, iPP crystallizes at higher temperatures during non-isothermal crystallization [41]. The crystallization enthalpy (ΔH_c) of ABS/PP blends increases with increasing the amount of PP and tends to be reduced in the graphene/ABS/PP nanocomposites (Table II).

According to An et al. [37] and Milani et al. [22], [34], the melting transition temperature (T_m) and crystallinity remain intact, the melting endothermic peak area (ΔH_m) and crystallization exothermic peak area (ΔH_c) decrease, whereas the crystallization temperature (T_c) is increased with the increment of graphene content in PP. Polschikov et al. [30] showed that this effect is stronger in the case of composites containing sonicated graphene nanoplatelets, due to the larger specific surface area of ultrasonically treated particles inside the composite. However, Achaby et al. [32] observed an increase in the crystallization temperature, but also an increase of crystallinity, crystallization enthalpy and melting temperature of PP, by adding graphene nanosheets. Song et al. [38] recorded an increase of the crystallization peak temperature and the crystallinity of PP, gradually with increasing the concentration of PP-coated graphene. Thereby, they considered that graphene can also act as seeds to induce the crystallization of PP.

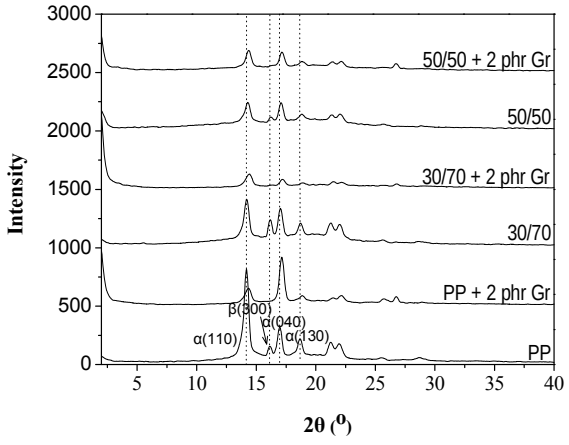

Fig. 1 XRD patterns of PP, 30/70 and 50/50 w/w ABS/PP blends and their graphene nanocomposites

Furthermore, the effect of graphene's addition to the *β*-phase of PP in ABS/PP blends was examined by XRD analysis (Fig. 1). PP and its blends present peaks at diffraction angles 2θ of 14°, 16.8°, 18.6°, 21.2° and 21.9° corresponding to the 110, 040, 130, 111 and the 131 and 040 lattice planes respectively of *α*-PP [8]. Moreover, the pure PP and PP-rich blends with ABS present a peak at 2θ=16.2°, which corresponds to the 300 lattice plane of *β*-crystals. The intensity of peak corresponding to *β*-PP of 30/70 ABS/PP blends is higher than that of neat PP and 50/50 w/w ABS/PP blend. The incorporation of graphene in PP and ABS/PP blends induces changes in their crystal conformation, resulting in the complete disappearance of the *β*-crystal form, which leads to *α*-PP. Similar observations were reported by Achaby *et al.* [32].

Also, a more detailed examination of the diagram can reveal a weak peak at about 26.5° in graphene/ABS/PP nanocomposites, characteristic of the spacing between graphene layers, corresponding to the 002 plane [22]. This peak can be attributed to the small extent of restacking of graphene nanosheets during melt mixing, because of Van der Waals interactions between adjacent sheets.

As it can be seen from Table III, PP exhibits superior thermal stability characteristics than ABS. The thermal degradation mechanism of their blends takes place in two stages. The first corresponds to the thermal degradation of ABS phase, whereas the second to that of PP phase. The addition of graphene into the investigated systems does not seem to affect their thermal degradation mechanism (Fig. 2).

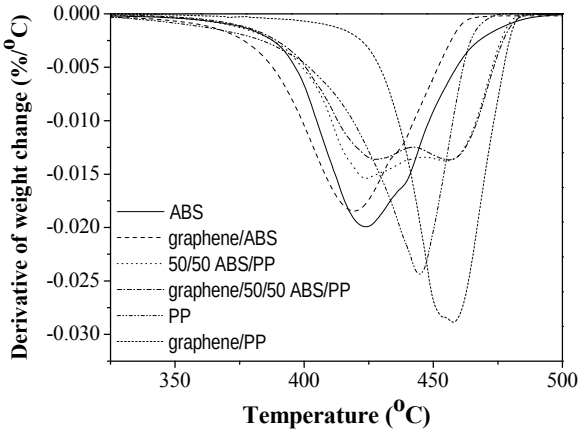

Fig. 2 Derivative of weight change versus temperature of ABS/PP blends and their nanocomposites with graphene

ABS/PP blends at 70/30 and 50/50 w/w present similar values of onset degradation temperature (T_{onset}) with that of pure ABS. The addition of graphene nanosheets into the ABS matrix causes reduction of its T_{onset}, whereas it increases the T_{onset} of pure PP. In ABS/PP blends, the incorporation of graphene does not have any significant effect on this characteristic temperature.

The 30/70 w/w ABS/PP blends present the higher temperature of maximum degradation rate, T_{peak}, being even higher than that of pure PP. The addition of graphene

nanosheets in PP matrix increases the maximum degradation rate temperature (T_{peak}). Achaby et al. [32] found that the addition of graphene nanosheets to PP increases the temperature for 5 and 15 % weight loss, as well as the maximum decomposition temperature. Furthermore, the residue of graphene/ABS/PP nanocomposites is improved in comparison with that of non-reinforced ABS/PP blends.

The addition of fillers into organic polymers can improve their thermal degradation stability because of the thermal isolation effect and the mass transport barrier effect. The graphene sheets hinder the diffusion of volatile decomposition products within the nanocomposites matrix [33].

TABLE III
THERMAL PROPERTIES OF ABS/PP BLENDS

Graphene (phr)	ABS/PP (w/w)				
	100/0	70/30	50/50	30/70	0/100
T_{onset} (°C)					
0	401.6 ±1.14	399.8 ±1.54	402.9 ±1.02	412.9 ±0.05	422.4 ±3.39
2	394.6 ±1.53	399.2 ±0.13	401.9 ±0.57	413.9 ±1.04	439.3 ±0.59
T_{peak} (°C)					
0	423.6 ±0.23	424.1 ±1.27	424.2/456.5 ±0.29/±2.10	458.0 ±1.64	445.1 ±3.41
2	420.1 ±1.12	423.9 ±0.76	427.2/455.6 ±0.62/±0.54	457.0 ±1.15	457.9 ±0.31
Residue (%)					
0	1.71 ±0.14	4.02 ±0.82	2.20 ±0.70	3.35 ±0.24	3.21 ±0.67
2	5.43 ±1.66	6.61 ±1.17	6.89 ±0.81	5.28 ±0.31	5.35 ±0.87

According to Table IV, ABS shows higher tensile strength and modulus of elasticity, but lower tensile strain compared to PP. Also, it seems that the tensile strength of ABS/PP blends is closer to that of PP, whereas the tensile strain of ABS/PP blends is much lower compared with that of their components. The Young's modulus decreases as PP concentration increases.

TABLE IV
TENSILE PROPERTIES OF ABS/PP BLENDS

Graphene (phr)	ABS/PP (w/w)				
	100/0	70/30	50/50	30/70	0/100
Tensile strength (MPa)					
0	46.77 ±0.22	29.97 ±0.95	35.31 ±0.69	36.53 ±0.67	35.36 ±0.47
2	48.45 ±1.46	29.75 ±1.36	35.53 ±1.40	37.13 ±0.24	40.32 ±0.23
Young's Modulus (MPa)					
0	2105.42 ±70.44	1882.52 ±16.25	1694.24 ±42.38	1730.07 ±64.19	1408.43 ±29.38
2	2429.10 ±49.25	2105.23 ±1.49	2197.91 ±25.69	2012.36 ±59.68	2014.50 ±60.07
Tensile strain at maximum load (%)					
0	13.21 ±3.15	2.65 ±0.05	4.24 ±0.63	8.02 ±1.63	25.15 ±4.04
2	6.45 ±2.07	2.76 ±0.54	3.57 ±0.56	4.86 ±0.35	15.09 ±2.67

The addition of graphene slightly improves the tensile strength of pure ABS, but significantly that of pure PP, whereas it does not obviously affect the tensile strength of their blends, probably due to the limited miscibility. In addition, it improves the elastic modulus and reduces the tensile strain of ABS/PP blends, at all the investigated compositions and mainly those of pure PP.

The improvement of mechanical properties can be attributed to the large aspect ratio, as well as to the high intrinsic mechanical characteristics and the rigidity of graphene nanosheets.

An increase of tensile strength and Young's modulus and a decrease of the elongation at break of PP by the incorporation of graphene nanosheets, have been reported by Milani et al. [22], An et al. [37] and Achaby et al. [32]. Also, Song et al. [38] observed an increase of tensile strength and Young's modulus of PP nanocomposites containing 1 wt% PP-coated graphene as a filler, due to the homogeneous dispersion of graphene nanosheets and the effective load transfer from the matrix to graphene because of their strong interfacial adhesion. Similar observations have also been reported for ABS reinforced with graphene functionalized by octadecylamine [33].

IV. CONCLUSIONS

The incorporation of graphene into ABS/PP blends significantly improves their tensile elastic modulus, whereas it increases their crystallization temperature and the amount thermal degradation residue. The thermomechanical properties of graphene/ABS/PP nanocomposites could be enhanced by adding the appropriate compatibilizer or by functionalizing the graphene nanosheets.

ACKNOWLEDGMENT

We would like to acknowledge the Bodossaki Foundation for the scholarship to Ms. Triantou PhD.

REFERENCES

[1] S. N. Maiti, V. Agarwal, A. K. Gupta, "Melt rheological behavior of PP–SAN blend," J. Appl. Polym. Sci., vol. 43, pp. 1891-1900, 1991.
[2] A. C. Patel, R. B. Brahmbhatt, B. D. Sarawade, S. Devi, "Morphological and mechanical properties of PP/ABS blends compatibilized with PP-g-acrylic acid," J. Appl. Polym. Sci., vol. 81, pp. 1731-1741, 2001.
[3] H. G. Lee, Y.-T. Sung, Y. K. Lee, W. N. Kim, H. G. Yoom, H. S. Lee, "Effects of PP-g-MAH on the mechanical, morphological and rheological properties of polypropylene and poly(acrylonitrile-butadiene-styrene) Blends," Macromol. Research, vol. 17, pp. 417-423, 2009.
[4] P. Xiang-Fang, P. Jun, X. Xiao-li, T. Lih-Sheng, "Effect of organoclay on the mechanical properties and crystallization behaviors of injection-molded PP/ABS/montmorillonite nanocomposites," ANTEC, pp. 1105-1108, 2009.
[5] C. Markin, H. L. Williams, "Polypropylene/ABS terpolymer blends. mixing and mechanical properties," J. Appl. Polym. Sci., vol. 25, pp. 2451-2466, 1980.
[6] A. K. Gupta, A. K. Jain, S. N. Maiti, "Studies on binary and ternary blends of polypropylene with ABS and LDPE. I. Melt rheological behavior," J. Appl. Polym. Sci., vol. 38, pp. 1699-1717, 1989.
[7] A. K. Gupta, A. K. Jain, B. K. Ratman, S. N. Maiti, "Studies on binary and ternary blends of polypropylene with ABS and LDPE. II. Impact and tensile properties," J. Appl. Polym. Sci., vol. 39, pp. 515-530, 1990.
[8] Q. Shu, X. Zou, W. Dai, Z. Fu, "Formation of β-iPP in isotactic polypropylene/acrylonitrile–butadiene–styrene blends: Effect of resin

type, phase composition, and thermal condition," J. Macromol. Sci., Part B: Physics, vol. 51, pp. 756–766, 2012.
[9] C. Wang, Z. Zhang, Y. Du, J. Zhang, K. Mai, "Effect of acrylonitrile–butadiene–styrene copolymer (ABS) on β-nucleation in β-nucleated polypropylene/ABS blends," Polym. Bull., vol. 69, pp. 847–859, 2012.
[10] M. Frounchi, R. P. Burford, "State of compatibility in crystalline polypropylene/ABS amorphous terpolymer thermoplastic blends. Effect of styrenic copolymers as compatibilisers," Iran. J. Polym. Sci. and Technol., vol. 2, pp. 59-68, 1993.
[11] E. Arroyo, C. Guerrero, V. Gonzalez, "Blends of ABS and iPP," ANTEC
[12] Y. K. Lee, J. B. Lee, D. H. Park, W. N. Kim, "Effects of accelerated aging and compatibilizers on the mechanical and morphological properties of polypropylene and poly(acrylonitrile-butadiene-styrene) blends", J. Appl. Polym. Sci., vol. 127, pp. 1032-1037, 2013.
[13] C. K. Kum, Y.-T. Sung, Y. S. Kim, H. G. Lee, W. N. Kim, H.S. Lee, H.G. Yoon, "Effects of compatibilizer on mechanical, morphological, and rheological properties of polypropylene/poly(acrylonitrile-butadiene-styrene) blends," Macromol. Research, vol. 15, pp. 308-314, 2007.
[14] A. C. Patel, R. B. Brahmbhatt, S. Devi, "Mechanical properties and morphology of PP/ABS blends compatibilized with PP-g-2-HEMA," J. Appl. Polym. Sci., vol. 88, pp. 72-78, 2003.
[15] Y. Wang, Q. Zhang, Q. Fu, "Compatibilization of immiscible poly(propylene)/polystyrene blends using clay", Macromol. Rapid Commun., vol. 24, issue 3, pp. 231-235, 2003.
[16] B. Chen, J.R.G. Evans, "Mechanical properties of polymer-blend nanocomposites with organoclays: Polystyrene/ABS and high impact polystyrene/ABS", J. Polym. Sci., Part B: Polym. Phys., vol. 49, issue 6, pp. 443-454, 2011.
[17] C. C. Ibeh, N. Baker, D. Lamm, S. Wang, D. Weber, J. Oplonitnik, ANTEC conference proceedings 5, pp. 1893-1897, 2005.
[18] Y. T. Sung, Y. S. Kim, Y. K. Lee, W. N. Kim, H. S. Lee, J. Y. Sung, H. G. Yoon, "Effects of clay on the morphology of poly(acrylonitrile-butadiene-styrene) and polypropylene nanocomposites," Polym. Eng. Sci., vol. 47, pp. 1671-1677, 2007.
[19] B. Panda, A. R. Bhattacharyya, A. R. Kulkarni, "Ternary polymer blends of polyamide 6, polypropylene and acrylonitrile-butadiene-styrene: Influence of multi walled carbon nanotubes on phase morphology, electrical conductivity, and crystallization," Polym. Eng. Sci., vol. 51, pp. 1550-1563, 2011.
[20] R. A. Khare, A. R. Bhattacharyya, A. R. Kulkarni, "Melt-mixed polypropylene/acrylonitrile-butadiene-styrene blends with multiwall carbon nanotubes: Effect of compatibilizer and modifier on morphology and electrical conductivity," J. Appl. Polym. Sci., vol. 120, pp. 2663–2672, 2011.
[21] R. A. Khare, A. R. Bhattacharyya, A. R. Kulkarni, M. Saroop, A. Biswas, "Influence of multiwall carbon nanotubes on morphology and electrical conductivity of PP/ABS blends," J. Polym. Sci.: Part B: Polym. Physics, vol. 46, pp. 2286–2295, 2008.
[22] M. Milani, R. Ouijada, N. R. S. Basso, A. P. Graebin, G. B. Galland, "Influence of the graphite type on the synthesis of polypropylene/graphene nanocomposites," J. Polym. Sci., Part A: Polym. Chem.,vol. 50, pp. 3958-3605, 2012.
[23] C. I. Ferreira., C. Dal Castel., M. A. S. Oviedoc, R. S. Mauler., "Isothermal and non-isothermal crystallization kinetics of polypropylene/exfoliated graphite nanocomposites," Thermochim. Acta, vol. 553, pp. 40– 48, 2013.
[24] P. Steurer, R. Wissert, R. Thomann, R. Mülhaupt, "Functionalized graphenes and thermoplastic nanocomposites based upon expanded graphite oxide," Macromol. Rapid Commun., vol. 30, pp. 316–327, 2009.
[25] S. Zhao, F. Chen, C. Zhao, Y. Huang, J.-Y. Dong, C. C. Han, "Interpenetrating network formation in isotactic polypropylene/graphene composites," Polymer, vol. 54, pp. 3680-3690, 2013.
[26] G. Gedler, M. Antunes, V. Realinho, J. L. Velasco, "Novel polycarbonate-graphene nanocomposite foams prepared by CO_2 dissolution," IOP Conf. Ser.: Mater. Sci. Eng., vol. 31, 2012.
[27] G. Gedler, M. Antunes, V. Realinho, J. L. Velasco, "Thermal stability of polycarbonate-graphene nanocomposite foams," Polym. Degrad. Stab., vol. 97, pp. 1297-1304, 2012.
[28] P. Song, L. Liu, S. Fu, Y. Yu, C. Jin, Q. Wu, Y. Zhang, Q. Li, "Striking multiple synergies created by combining reduced graphene oxides and carbon nanotubes for polymer nanocomposites," Nanotechnology, vol. 24, no. 12, 2013.
[29] B. Shen, W. Zhai, M. Tao, D. Lu, W. Zheng, "Chemical functionalization of graphene oxide toward the tailoring of the interface in polymer composites," Compos. Sci. Technol., vol. 77, pp. 87-94, 2013.
[30] S. V.Polschikov, P. M. Nedorezova, A. N. Klyamkina, A. A. Kovalchuk, A. M. Aladyshev, A. N. Shchegolikhin, V. G. Shevchenko, V. E. Muradyan, "Composite materials of graphene nanoplatelets and polypropylene, prepared by in situ polymerization," J. Polym. Sci., vol. 127, issue 2, pp 904-911, Jan. 2013.
[31] H. J. Park, J. Meyer, S. Roth, V. Skákalová, "Growth and properties of few-layer graphene prepared by chemical vapor deposition," Carbon, vol. 48, pp. 1088-1094, 2010.
[32] M. E. Achaby, F. E. Arrakhiz, S. Vaudreuil, A. K. Qaiss, M. Bousmina, O. Fassi-Fehri, "Mechanical, Thermal, and Rheological Properties of Graphene-Based Polypropylene Nanocomposites Prepared by Melt Mixing," Polym.Compos., vol. 33, issue 5, pp. 733-744, May 2012.
[33] C. Heo, H.-G. Moon, C.-S. Yoon, J.-H. Chang, "ABS Nanocomposite films based on functionalized-graphene sheets", J. Appl. Polym. Sci., vol. 124, pp. 4663–4670, 2012.
[34] M. Milani, D. González, R. Ouijada, N. R. S. Basso, M. L. Cerrada, D. Azambuja, G. B. Galland, "Polypropylene/graphene nanosheet nanocomposites by in situ polymerization: synthesis, characterization and fundamental properties," Comp. Sci. Technol., vol. 84, pp. 1-7, 2013.
[35] V. G. Shevchenko, S. V. Polschiko, P. M. Nedorezova, A. N. Klyamkina, A. N. Shchegolikhin, A. M. Aladyshev, V. E. Muradyan, "In situ polymerized poly(propylene)/graphene nanoplatelets nanocomposites: Dielectric and microwave properties," Polymer, vol. 53, pp. 5330-5335, 2012.
[36] J.-Z. Xu, C. Chen, Y. Wang, H. Tang, Z.-M. Li, B. S. Hsiao, "Graphene Nanosheets and Shear Flow Induced crystallization in isotactic polypropylene nanocomposites," Macromolecules, vol. 44, pp. 2808–2818, 2011.
[37] J.-E. An, G. W. Jeon, Y. G. Jeong, "Preparation and properties of polypropylene nanocomposites reinforced with exfoliated graphene", Fibers Polym., vol. 13, no. 4, pp 507-514, 2012.
[38] P. Song, Z. Cao, Y. Cai, L. Zhao, Z. Fang, S. Fu, "Fabrication of exfoliated graphene-based polypropylene nanocomposites with enhanced mechanical and thermal properties", Polymer, vol. 52, pp. 4001-4010, 2011.
[39] J. Dai, Y. Shen, J.-H. Yang, T. Huang, N. Zhang, Y. Wang, "Crystallization and melting behaviors of polypropylene admixed by graphene and β-phase nucleating agent", Colloid Polym. Sci., pp. 1-11, 2013.
[40] J. Ma, Q. Meng, I. Zaman, S. Zhu, A. Michelmore, N. Kawashima, C. H. Wang, H.-C. Kuan, "Development of polymer composites using modified, high-structural integrity graphene platelets," Comp. Sci. Technol., vol. 91, pp. 82–90, 2014.
[41] J.-B. Chen, J.-Z. Xu, H. Pang, G.-J. Zhong, L. Xu, H. Tang, J.-H. Tang, Z.-M. Li, "Crystallization of Isotactic Polypropylene inside Dense Networks of Carbon Nanofillers", J. Appl. Polym. Sci., vol. 131, issue 6, 2014.